



Shahrood University of
Technology



Iranian Society of
Mining Engineering
(IRSM)

Fractal Modeling of Geochemical Mineralization Prospectivity Index based on Centered Log-Ratio Transformed Data for Geochemical Targeting: a Case Study of Cu Porphyry Mineralization

Hossein Mahdianfar^{1*} and Amir Salimi²

1. Department of mining engineering, University of Gonabab, Iran

2. Mining Engineering Group, Faculty of Engineering, University of Zanjan, Zanjan, Iran

Article Info

Received 21 June 2022

Received in Revised form 18
August 2022

Accepted 7 September 2022

Published online 7 September
2022

[DOI:10.22044/jme.2022.12024.2197](https://doi.org/10.22044/jme.2022.12024.2197)

Keywords

Anomaly mapping

Outlier detection

Fractal modeling

Geochemical model

Abstract

This work aims to investigate the geochemical signatures of the Cu porphyry deposit in the Dalli area using the geochemical soil samples. At the first step, the geochemical data was opened using the Centered Log-Ratio (CLR) transform method. Then those outlier samples that reduce the accuracy of the geochemical models were detected and removed using the Mahalanobis Distance (MD) method. We applied the Principal Component Analysis (PCA) and Geochemical Mineralization Prospectivity Index (GMPI) methods on the cleaned transformed geochemical dataset. The PCA method identified five principal components (PCs), from which PC1 including Cu, Au, and Mo, are specified as the mineralization factor (MF). The GMPI approach can improve the multivariate geochemical signature in geochemical mapping. Hence, the GMPI values of the samples were calculated based on the score values of MF (Cu, Au, Mo). The results convey that the large values of GMPI (MF) (Cu, Au, Mo) strongly correlate with the quartz diorite porphyry rocks and potassic alteration zones. The GMPI (MF) (Cu, Au, Mo) index was modeled using the Concentration-Number (C-N) fractal method. The C-N fractal model identified four geochemical populations based on the different fractal dimensions. The geochemical anomaly map of GMPI (MF) (Cu, Au, Mo) was delineated using these classified populations. The obtained promising areas were validated adequately by more detailed exploration works and deep drilled boreholes as well. The Cu-Au mineralization potential parts are appropriately mapped by this hybrid method. The results obtained demonstrate that this scenario can be adequately used for geochemical mapping on local scales.

1. Introduction

Commercially mineral deposits are generally prospected using the geoscience datasets such as the geological, geochemical, and geophysical data. Concerning the conceptual exploration models of ore deposit types, the relevant data is gathered and processed to produce the spatial geo-information. This valuable information aims to specify the anomaly areas that have more chance of associating with a probable mineral deposit [1, 2]. The geochemical anomalies are the enriched

concentration areas of some indicator or pathfinder elements related to the ore-forming. The importance of geochemical anomaly mapping is undeniable for mineral prospectivity mapping [3, 4]. The anomalous areas in various media (e.g. soils, rocks, and stream sediments) are distinguishable from the background when the threshold values are correctly identified [1, 5]. The geochemical anomaly mapping and geochemical society discrimination have always been fundamental challenges in a geochemical data

✉ Corresponding author: Hssn.Mahdianfar@gmail.com (H. Mahdianfar).

analysis [6–8]. The threshold value modeling can be carried out via two groups of methods: traditional and modern types, which are also known as the frequency-based and spatial frequency-based approaches, respectively [1, 6, 9, 10].

In addition to data frequency, which is merely an essential parameter for traditional approaches, modern methods consider some other types of geo-information. Geographical coordinate of samples, geometrical aspects like shape, orientation, and fractal dimensions of geochemical anomalies are the most critical spatial features taken into account by modern methods.

The geochemical anomaly mapping methods are based on the uni-element and multi-element analysis approaches.

PCA, as a familiar multi-element technique, has been frequently applied to study the inter-element relationships of the geochemical datasets [11–16]. The inter-element variations that reflect the dominant geochemical process can be recognized using PCA [1]. PCA has been utilized for the geochemical interpretation and identification of paragenetic elements of mineralization in the spatial domain [11, 17], frequency domain [18], and wavelet domain [19, 20]. In this work, the extracted MF from PCA was modeled using GMPI.

The GMPI introduced by Yousefi *et al.* is a technique for fuzzifying the geochemical data [21]. They demonstrated that applying GMPI as the fuzzy weight of samples could increase and enhance the geochemical anomaly intensity. Some studies have applied GMPI as evidential scores to improve geochemical prospecting [22–26]. The GMPI values as the multi-element signatures can be modeled using the anomaly separation methods such as fractal geometry approaches.

The fractal/multi-fractal methods have been extensively applied to classify the geochemical data based on the fractal geometry dimensions. The scale-independency of geochemical patterns allows those areas with various intensities, in terms of element concentration, to be identified by the fractal geometry theory [10, 27–30]. Fractal-based geochemical data processing has been accomplished by various techniques such as the number-size model [31], concentration–number (C-N) [32, 33], concentration–area [27, 34, 35], concentration–distance [36], spectrum–area [37–40], and concentration–volume [41]. The combination of fractal models with machine learning methods has

also been used for anomaly mapping [42, 43]. Hassanpour and Afzal [44] have proposed the C-N fractal method for modeling the geochemical data and separating the geochemical anomalies. Shahbazi *et al.* have demonstrated that the mineralization phases could be determined by the C-N multi-fractal modeling [45].

Pre-processing of data is also not being ignored before the data processing phase. Outlier values detection is an essential task for the pre-processing of geochemical data, performed by various approaches.

Since the concentration values of geochemical samples are compositional data, interpretation of this type of data in the Hilbert space using the standard statistical analysis methods does not result in desirable and accurate outputs [46]. It has been demonstrated that statistical correlation analysis of geochemical data can produce more informative results when the log-ratio transformed data is utilized [47]. Simply speaking, when a transformation algorithm is firstly performed on data, and after that, the data correlation is calculated; the results reflect much better information about groups of chemical elements of the studied area [46].

The aim of this work is geochemical anomaly separation by integrating some classic and modern analytical methods. In the first step, the geochemical composition data was opened and cleaned using the CLR transform approach and Mahalanobis Distance (MD) method, respectively. The pre-processing phase was followed by performing PCA on the previous transformed data to extract more informative components. The GMPI method was applied to enhance the exploration probability on the regional scale. Still, in this investigation, we used this method for prospectivity mapping of Cu, Au, and Mo mineralization on the local scale. Then the fractal model was performed on the multivariate geochemical signature for classifying the GMPI (Cu, Au, Mo) and geochemical targeting. The principal aim of this investigation is to delineate multi-element anomalies of Cu, Mo, and Au in the local scale explorations using a hybrid method by integrating GMPI, PCA, and C-N fractal model based on the cleaned CLR transformed dataset.

2. Geological setting

Dalli area contains a porphyry mineralization type of Cu-Au, namely Dalli. The area, which is located

in the Markazi province of Iran, is a part of the west edge of the Uromieh-Dokhtar magmatic belt [48]. This belt that is extended about 400 Km from NW to SE of Iran, contains the alkaline and calc-alkaline intrusive-volcanic rocks and some important mines such as Sarcheshmeh, Meiduk, Darreh-Zereshk, Kahang, and Sungun [49].

The primary constructing rocks of the Dalli district are Eocene volcanic and pyroclastics formations including andesitic to basaltic lava and andesitic to rhyodacitic pyroclastics. These formations are intruded by Oligo-Miocene medium basic intrusive-igneous rocks (diorite, quartz diorite, and tonalite), and some volcanic rocks (andesite, ignimbrite, and porphyry andesite) can be locally seen (Figure 1). These formations due to the influence of hydrothermal solutions have been completely altered to the potassic, silicic, phillitic, argillic, and propylitic alterations at an area of about 3 by 6.5 Km [50]. The geological studies confirmed that the disseminated mineralization was mainly related to the potassic, silicic, and locally phillitic zones [51]. It was deposited during penetration of some intrusive quartz dioritic stocks and dykes to andesitic volcano rocks via a faulted zone with a width of 3 Km and an azimuth of 55°.

Dalli is divided into the northern and southern hills. The southern deposit is an area of about 190 m by 200 m. Its principal characteristic features are intensive potassic and locally phillitic and silica alteration zones due to the emplacement of a dioritic intrusion [50]. This hill includes outcrops of oxide-type minerals of Cu and Au, e.g. malachite, azurite, cuprite, hematite, and goethite. This zone, with an average grade of 1 ppm and 0.4% for Au and Cu, respectively, extends nearly to the depth of 50 m. The supergene zone, by strong chalcocite and malachite mineralization and about 3.5% and 1 ppm of Cu and Au, has formed at a depth of 50 m to 60 m (approximately 8 m). These zones are followed by a hypogene zone composed of approximately 0.65 ppm and 0.45% of Au and Cu. The evidence of ore minerals (chalcopyrite, pyrite, bornite, magnetite, and native gold) has been confirmed via drilled

boreholes up to 350 m. The reserve of the southern part, up to 350 m, has been estimated to be about 38 million tons containing 60 ppm and 0.45% of Au and Cu.

Dalli's northern mineralization has occurred in an area about twice of the southern hill. The supergene zone in the northern hill is weak compared to the south of region. The concentration of Au is the same in both parts but the northern area is weaker in terms of Cu concentration (about 0.2%). The northern deposit has been estimated to contain about 50 million tons of ores. According to the estimated reserve of the entire area, Dalli is classified as a world-class deposit [52, 53].

3. Methodology

3.1. CLR transform

The log-ratio transformation method is categorized as Additive Log-Ratio transformation (ALR), Centered Log-Ratio transformation (CLR), and Isometric Log-Ratio transformation (ILR) [35, 46]. The CLR method is preferred to eliminate the effect of the closed data due to some reasons [54]. For example, a useful fact to ignore the ALR is its dependency on personal experience [44-47], as well as ILR, is somewhat complicated, and interpretation of its outputs does not perform readily because of the dimensionality reduction of data [56-58].

CLR is a log-ratio transformation method. According to the CLR theory, the logarithm of variables is firstly calculated, then the result obtained for each variable is divided by the geometric mean of the same variable (Equation 1). Unlike ALR, not elimination of any variables is an advantage for CLR. However, the impossibility of many multivariate statistical analysis methods to utilize CLR's output can still be considered a significant disadvantage [54].

$$CLR(x) = \left[\ln \frac{x_i}{\sqrt[D]{\prod_{i=1}^D x_i}}, \dots, \ln \frac{x_D}{\sqrt[D]{\prod_{i=1}^D x_i}} \right] \quad (1)$$

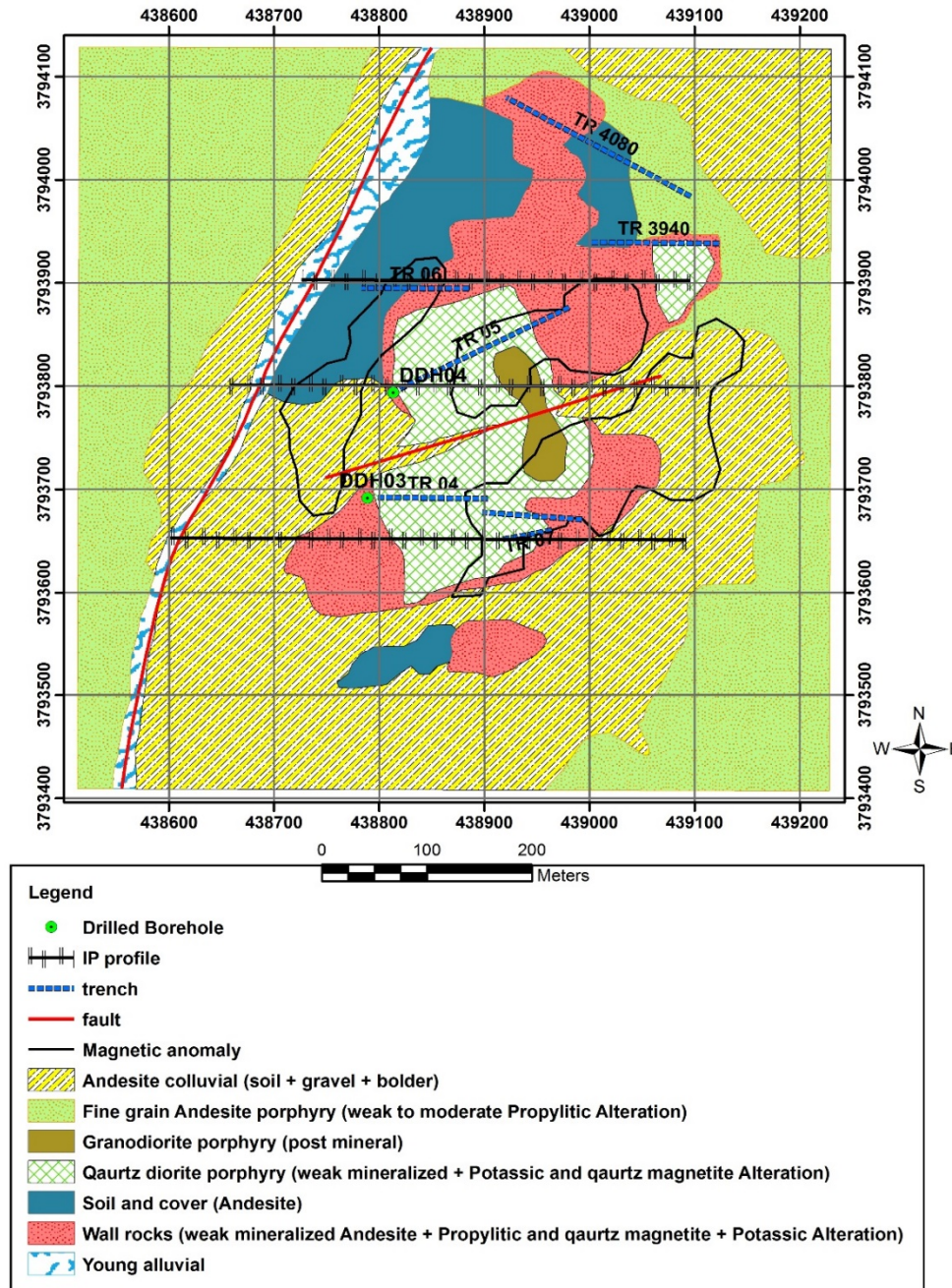


Figure 1. Geological map of northern part of the Dalli area (scale 1:1000: revised based on [52]).

3.2. Data cleaning

The outliers are the data that does not follow the general pattern of the majority of the data, and are far from the dataset. The outliers can increase error rates and create remarkable during the data processing statistical methods [59].

A popular multivariate distance measured based on the covariance matrix is MD. MD is calculated as the following equation:

$$MD_i = ((x_i - t)^T C^{-1} (x_i - t))^{1/2} \quad (2)$$

where x_i , t , and C are the multivariate samples, estimated multivariate location, and covariance matrix, respectively. The values almost have a chi-square distribution when the multivariate data is distributed normally. The multivariate outliers with large MD can be distinguished from the normal data based on the chi-square distribution [60].

A constant percentile of the χ^2 distribution is utilized to isolate the outliers from the non-outliers. The samples are separated into groups of outlier and normal data using the threshold value calculated by $\sqrt{\chi^2_{1-\alpha, v}}$. v is the degree of freedom of variables, and α is the significance level for a fixed quantile [61].

3.3. GMPI approach

GMPI is a technique introduced by Yousefi *et al.* [21] to transform scores of the PCA method into the fuzzy scale. The GMPI method has important advantages in geochemical prospecting. This multivariate approach reduces the dimensions of geochemical data, and detects the paragenetic and effective elements in the mineralization phase. The geological phenomena and geochemical societies can be interpreted using the results of GMPI [62]. PCA, a usual multivariate method to analyze the geochemical data, generates outputs known as the sample's score, which indicates the relative importance of each sample.

PCA as a multi-element analysis method has been applied to interpret the geochemical data in the spatial, frequency, and wavelet domains [15, 19, 63].

PCA applies the correlation matrix of all elements to determine the number of uncorrelated principal components (PCs) (equals to the number of elements), where the first and last PCs have the highest and least proportion of the total variance, respectively [1].

The mineralization factor can be detected and extracted using the rotated component matrix of PCA. The new score for each sample is calculated in the new rotated domain based on the Varimax. These absolute scores are considered new geochemical multi-element features [64, 65].

The obtained scores were applied to calculate GMPI using a logistic sigmoid function, as below [21]:

$$GMPI = \frac{e^{FS}}{1 + e^{FS}} \quad (3)$$

where FS is the score of each sample. It has been demonstrated that utilizing GMPI as the fuzzy weight of samples can increase and enhance the geochemical anomaly intensity [21, 23–25, 66, 62].

3.4. Concentration-number (C-N) fractal method

The fractal/multi-fractal geometry theory is applied to analyze scale-independent and self-similar shapes or phenomena [63]. If geochemical landscapes tend to pose self-similar and scale-independent properties [64], thus can be analyzed by the theory of non-Euclidean fractal geometry. As a result, the anomalous areas are distinguished from the background based on the fractal dimensions [1]. Since the 1980s, various fractal/multi-fractal-based approaches have been established in various geoscience fields, namely geology, petrology, geophysics, geochemistry, etc. [7, 65, 66]. Concentration-Number (C-N) multifractal method has been frequently used to analyze the geochemical samples and separate them into the background and anomalous areas [32]. This model has been constructed on the relation as below:

$$N(\geq \rho) \propto \rho^{-\beta} \quad (4)$$

where $N(\geq \rho)$ indicates the number of samples having concentration values greater than the concentration (ρ), and the fractal dimension is β . When the exponential relationship between N and ρ is plotted on a log-log graph, the slope of the resulted straight line is the fractal dimension (β) of that individual concentration (ρ). In the simplest situation with two populations including one background and one anomalous area, two straight lines are formed with different slopes representing the two populations, namely anomaly and background with greater and lower slopes, respectively. Finally, the broken point of the lines is assigned to the threshold concentration value, which is applied to separate the background and anomalous areas [1].

4. Results and Discussion

For geochemical exploration in the Dalli area, 165 systematic soil samples (50×50 m) with a fraction of -200 were taken and analyzed for 45 elements by ICP-MS (Inductively Coupled Plasma Mass Spectrometry) in AMDEL Lab in Australia.

In this work, the CLR transform, MD, PCA, GMPI, and fractal geometry methods were performed on the geochemical data for mineral potential mapping. The flowchart of the applied scenario for geochemical data modeling is indicated in Figure 2.

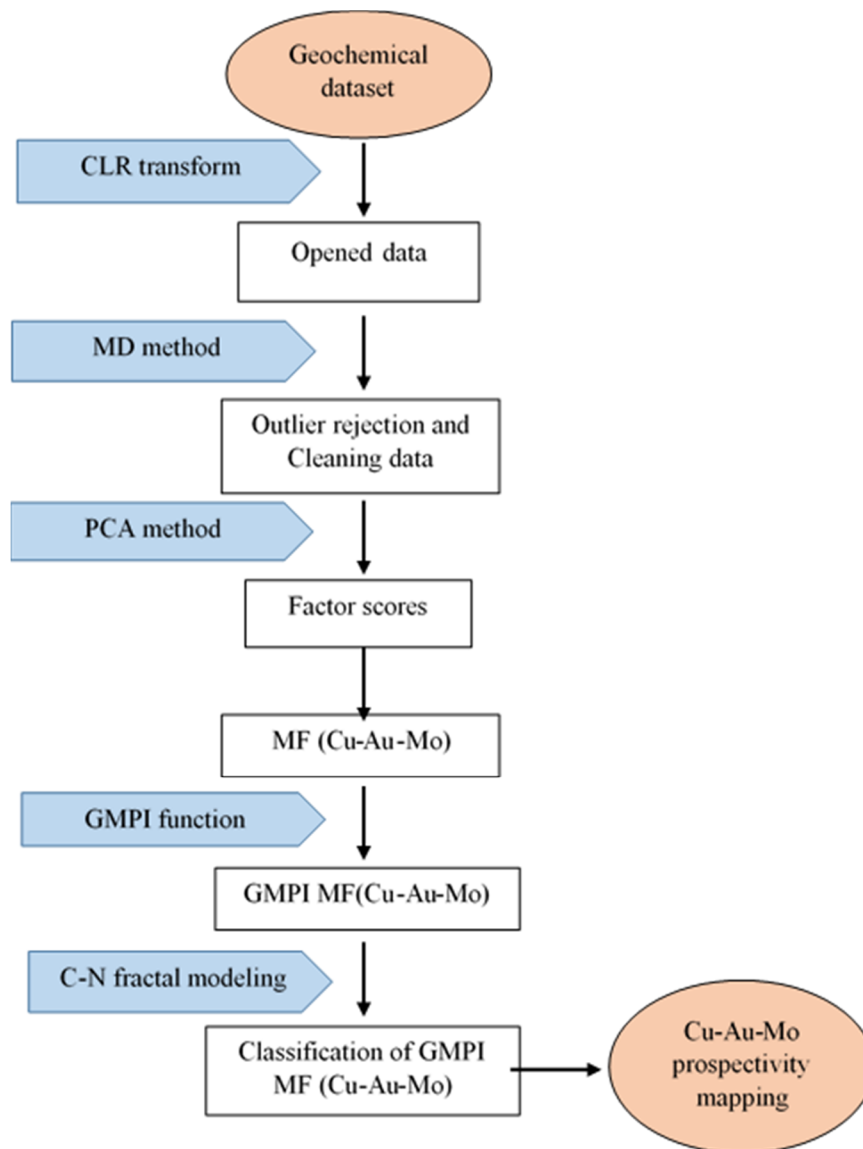


Figure 2. Flowchart of the applied scenario for geochemical anomaly mapping.

4.1. Cleaning of log-ratio transformed geochemical data

The geochemical data are known as the compositional data. Hence, misleading interpretations may be created when applying standard statistical analysis to the original dataset. Accordingly, CLR transform based on Equation 1 is used on raw assays to achieve the correct representation of relationships between the elements in this investigation.

The outlier values strongly affect multivariate statistical results and provide unrealistic information from the dataset. To overcome this issue and to clean

the log-ratio transformed data, the MD method was performed for the detection of normal and outlier data. The MD follows a χ^2 distribution and can effectively separate the most excessive outliers.

Twelve samples were detected as the outlier data from 163 samples based on significance level 0.001, which gives a 99.9% quantile. This threshold properly facilitated outlier removal in multivariate geochemical data. The sampling grid of geochemical data containing outlier and non-outlier (normal) data and the spatial distribution of outliers are depicted in Figure 3.

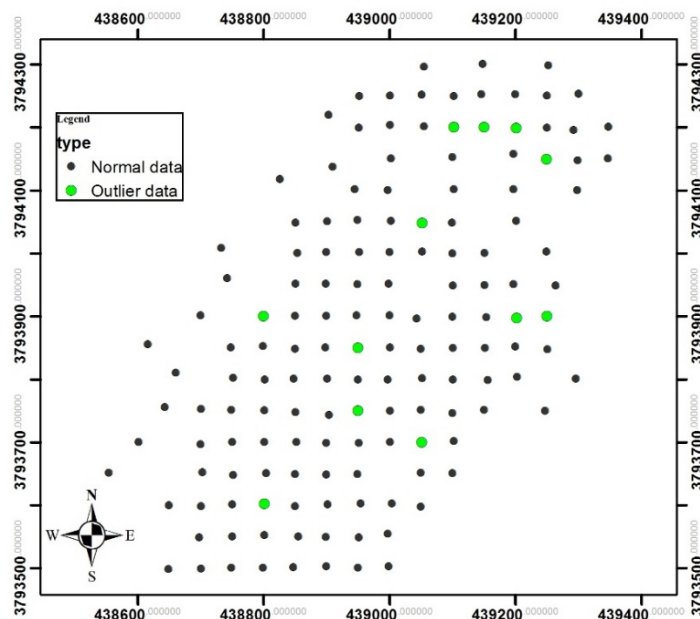


Figure 3. Location of geochemical samples (normal and outlier samples are shown).

The MD values of the geochemical samples and separated normal and outlier samples based on the threshold of $\sqrt{\chi^2_{0.999,28}}$ are shown in Figure 4.

4.2. Extraction of MF using PCA

Distinguishing the mineralization and paragenetic elements and recognizing the relationships between the elements are vital for the improvement of multivariate geochemical prospectivity mapping. After opening the geochemical data using CLR transformation and cleaning the dataset from outliers, the PCA method was applied to extract the principal factors related to the 29 logarithmic elemental concentration data. The attributes of MF and paragenetic elements can be identified using PCA. The factor scores of samples were calculated using the Varimax rotation and Kaiser normalization methods. For this aim, firstly, the Kaiser normalization was performed on the CLR transformed data, then the Varimax method was used for rotating axes. PCA appropriately reduced the dimensions of features and created PCs in a new space. PCA method extracted five PCs from 29 initial features based on the eigenvalues of more than one, and the other components were ignored. The rotated component matrix related to the elements created by PCA is shown in Table 1. Rotation was converged in 6 iterations. The mineralization elements of Cu, Au,

and Mo affect PC1 with a negative sign. PC 1, 2, and 3 have been plotted in a new rotated space, and the mineralization elements of Cu, Au, and Mo have been discriminated in Figure 5.

The variances and cumulative variances of the deriving PCs are shown in Figure 6. These five PCs contain 81% of the total variance related to the dataset.

Figure 6 indicates a decreasing trend for the variance values from PC5 to PC1 that demonstrates that PC1 has an essential role in the geological and mineralization phenomena in this area. The factor scores of elements greater than 0.6 were considered for analyzing the extracted PCs and their important elements. The mineralization elements of Au, Cu, and Mo play an essential role in constructing the first PC. The rotated component matrix indicates the absolute factor loadings of these elements in PC1 are more than 0.6. Hence, PC1, which shows 34% of the variance of the dataset, was detected as MF of Au, Cu, and Mo. The $MF_{(Au, Cu, Mo)}$ is more important out of the other PCs and includes the higher variations of the dataset. The mineralization elements of Au, Cu, and Mo hold negative loadings in MF. Figure 7 shows the negative factor loadings of elements in PC1. The elements of Au, Cu, and Mo have no significant signature on the other PCs. $MF_{(Au, Cu, Mo)}$ as a multi-element index intensifies the geochemical anomaly signature, and improves the prospectivity mapping.

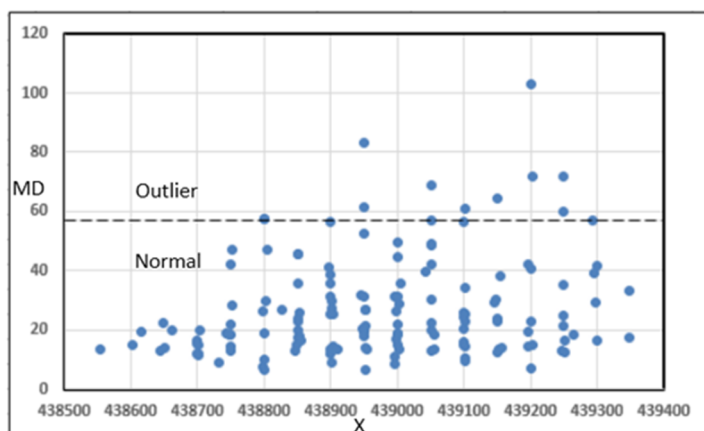


Figure 4. MD values of geochemical samples (normal and outlier samples are shown).

Table 1. Rotated component matrix created by PCA (mineralization elements of Cu, Au, and Mo affect PC1 with negative sign).

	Principal component				
	1	2	3	4	5
Au	-0.743	-0.232	0.486	0.068	0.166
Al	0.386	0.820	-0.169	-0.135	-0.148
As	0.753	-0.135	-0.136	-0.134	-0.164
B	0.801	0.036	-0.346	0.087	-0.054
Ba	0.143	0.742	-0.221	0.289	-0.036
Ca	0.366	0.170	-0.666	-0.067	0.457
Ce	0.160	-0.124	0.068	0.932	0.121
Co	0.620	0.504	-0.021	-0.315	-0.119
Cr	0.830	0.087	0.039	0.201	0.163
Cu	-0.772	-0.118	0.438	0.141	0.272
Fe	-0.233	0.405	0.750	-0.057	-0.010
Ga	0.011	0.837	0.170	-0.126	-0.124
K	0.062	0.719	0.214	0.271	0.356
La	0.107	-0.124	-0.022	0.928	0.119
Li	0.714	0.522	-0.296	0.185	-0.027
Mg	0.116	0.867	-0.075	0.036	0.388
Mn	0.845	0.303	0.191	0.068	-0.005
Mo	-0.657	0.214	0.245	0.060	-0.298
Na	0.399	0.677	0.010	-0.413	-0.216
Ni	0.928	0.072	-0.177	0.182	-0.002
P	-0.009	0.016	0.739	0.056	0.114
Pb	0.292	0.369	-0.025	-0.307	-0.723
Sc	-0.280	0.887	-0.076	0.013	-0.056
Sr	.585	.252	-.626	-.273	-0.046
Ti	-0.372	0.465	0.414	0.184	0.589
V	-0.129	0.702	0.517	-0.167	-0.031
Y	-0.036	0.443	0.107	0.763	-0.049
Zn	0.399	0.675	0.319	-0.051	-0.178
Zr	0.759	-0.093	0.128	0.163	-0.352

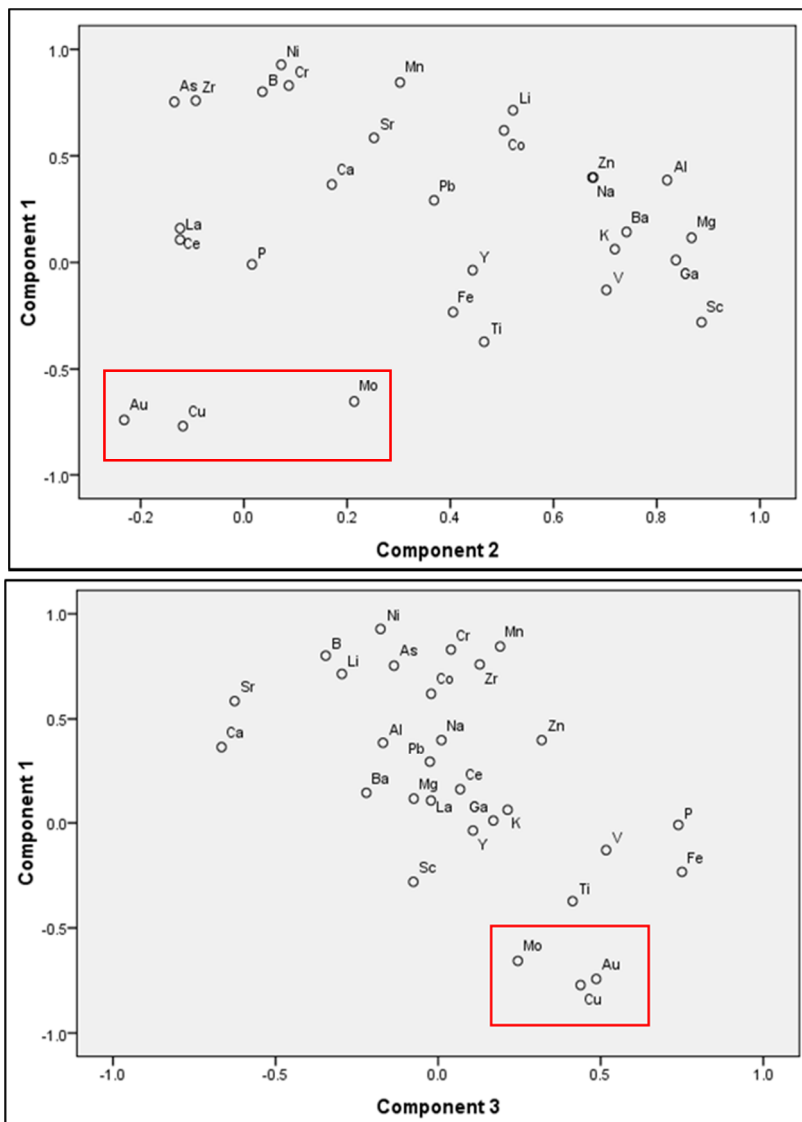


Figure 5. Component plots in rotated space for PC1, 2, and 3, mineralization elements were discriminated.

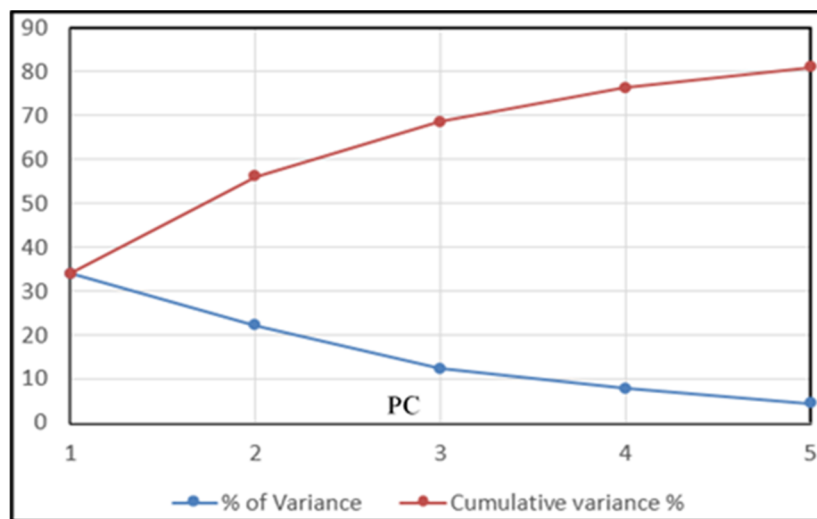


Figure 6. Variances and cumulative variances of deriving PCs from PCA.

The PC1 as $MF_{(Au, Cu, Mo)}$ was selected for calculating the GMPI values, and anomaly map was obtained based on the absolute factor scores of $MF_{(Au, Cu, Mo)}$.

PCA decreases the discrimination of geochemical societies, and intensifies the geochemical anomalies.

4.3. Fractal modeling of GMPI_(MF) for cleaned log-ratio data

The results of PCA indicate that mineralization paragenetic elements include Cu, Au, and Mo. Hence, PC1 as $MF_{(Au, Cu, Mo)}$ was selected for prospectivity mapping.

After identifying the PC containing the mineralization elements, multi-element MF was transformed into a new rotated space. The geochemical anomalies are improved and intensified using this transferring in this space.

The GMPI values were obtained using the following logistic sigmoid equation:

$$GMPI(MF_{(Au,Cu,Mo)}) = \frac{e^{-MF_{(Cu,Au,Mo)}}}{1 + e^{-MF_{(Cu,Au,Mo)}}} \quad (5)$$

The negative MF scores of samples were used for GMPI calculation because the mineralization elements of Au, Cu, and Mo hold negative loadings for MF in the rotated component matrix.

The GMPI values were interpolated by the Kriging method for geochemical mapping (Figure 8). This map indicates the spatial distribution of GMPI and the situation of promising areas. The GMPI results have detected a NE-SW trend for anomaly zones and precisely convey that high anomaly values have occupied the central part of the area. The GMPI model of MF as a multi-element geochemical signature based on the CLR transformed data can adequately highlight the potential areas for future detailed exploration.

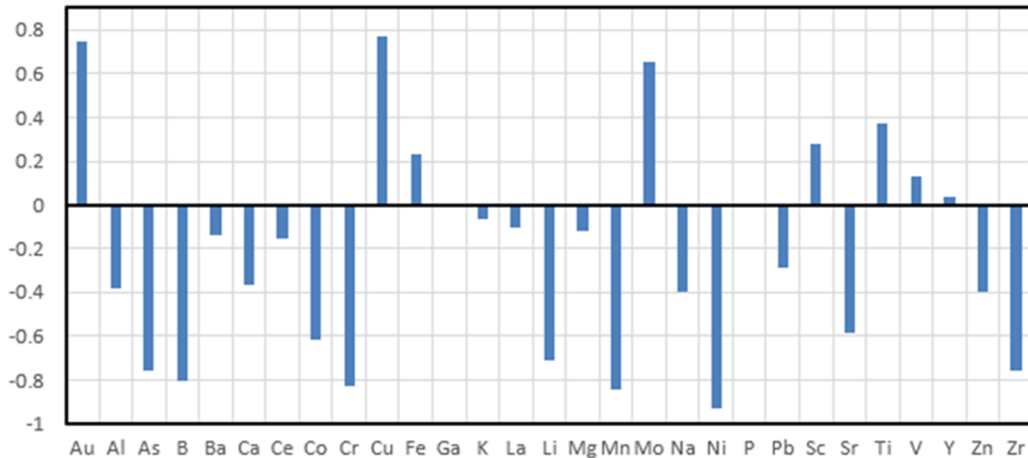


Figure 7. Factor loadings of elements in rotated component matrix relevant to MF obtained by PCA.

The obtained GMPI ($MF_{(Au, Cu, Mo)}$) values were categorized using C-N fractal modeling. Figure 9 illustrates four geochemical societies with multifractal nature for GMPI. In a logarithmic fractal plot, the slopes of fitted straight lines convey the fractal dimensions of various geochemical populations. The threshold values can also be obtained using the breakpoints in this diagram.

Three threshold values for GMPI ($MF_{(Au, Cu, Mo)}$) consisting of 0.815, 0.656, and 0.545 were identified in this log-log fractal plot. These thresholds separate four geochemical populations of background, weak anomaly, moderate anomaly, and high anomaly. The first class including the GMPI values less than 0.545 is related to the background population, and the other three classes are relevant to the geochemical anomalies.

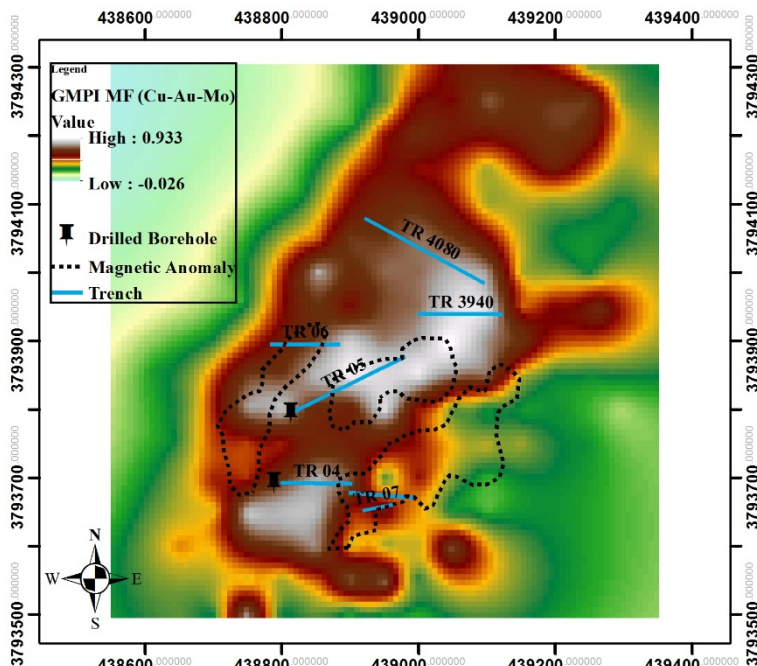


Figure 8. GMPI anomaly mapping based on MF_(Cu-Au-Mo).

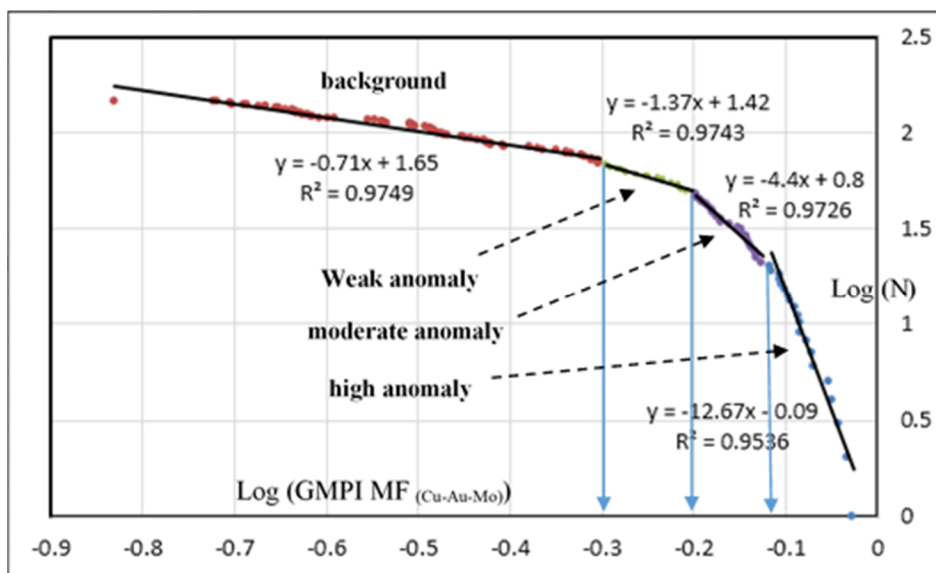


Figure 9. Log-log plot of C-N fractal modeling of GMPI (MF_(Cu-Au-Mo)).

The four geochemical populations of background, weak anomaly, moderate anomaly, and high anomaly were discriminated and mapped in Figure 10. This figure shows the multivariate geochemical prospectivity map obtained from C-N fractal modeling of GMPI MF (Cu-Au-Mo). The high anomalous area of GMPI is located in the central part of the district, which is proposed as a high potential area for detailed exploration in the future. The

moderate and weak anomalies have a distinctive NE-SW trend and cover more extensive parts of the studied area. The intermediate and high anomaly areas have the most important priority for deep explorations such as drilling boreholes and geophysical studies. Generally, the most promising parts with high mineralization potential are in the center of the area.

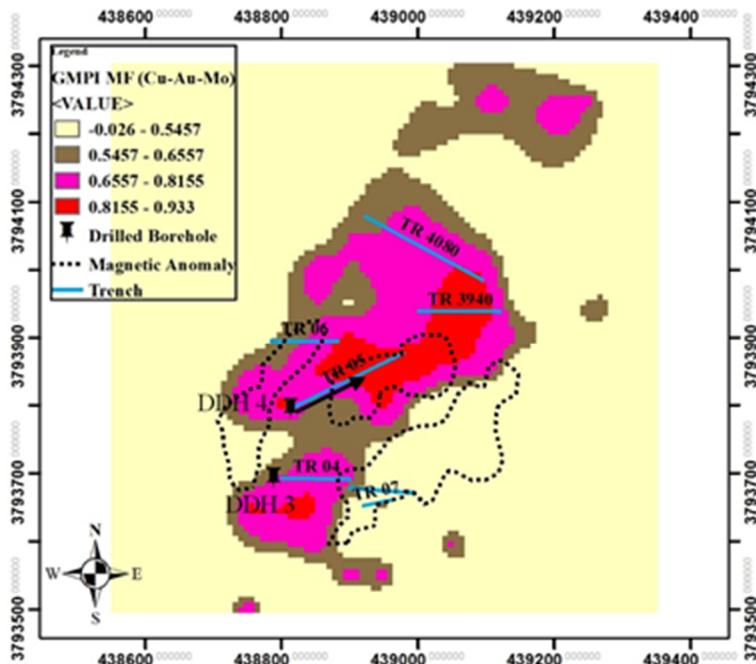


Figure 10. Multivariate prospectivity map obtained from C-N fractal modeling of GMPI MF_(Cu, Au, Mo).

4.4. Assessment of obtained promising targets

The fractal modeling of GMPI _(Cu, Au, Mo) indicated that there were moderate and high anomaly populations in CLR transformed dataset. These significant moderate and high anomalies have been extended in the central parts of the area. The field observations and detailed studies indicated an oxide zone with obvious Au and Cu mineralization outcrops in these anomaly parts. Several surface trenches were drilled on high potential targets for prospecting the alteration and mineralization and evaluating the anomaly areas.

Trench 04 (TR04) drilled on the anomaly area (Figure 10) includes the quartz diorite porphyry

rocks and a small extent of andesite rock. The high and moderate potassic and weak phillic and chlorite alterations were observed in this trench. In this part, we are facing a mineralized zone. The mineralization veinlets of malachite, silicified, and iron oxide are abundant. The grade of Au is even more than two ppm, and there is a high correlation between Cu and Au.

Trench 3940 (TR 3940) drilled in the northern part of the central anomaly (Figure 10) also confirms a mineralized zone in the obtained geochemical anomaly map. The concentration distribution of the Au and Cu elements is illustrated in Figure 11.

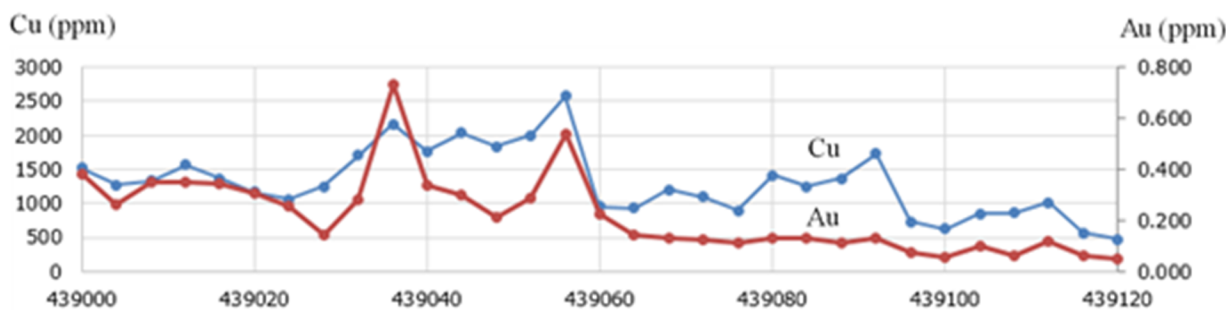


Figure 11. Concentration distribution of Au and Cu elements in trench 3940.

The two boreholes of DDH3 and DDH4 were designed and drilled based on the situation of surface mineralization and the trend of TR04 and TR05 (Figure 10).

These boreholes indicated that there were three mineralization zones consisting of supergene, transition, and hypogene at the depth. Like surface studies, the potassic and phillitic alterations are shown in quartz diorite porphyry, and andesite rocks have been altered to propylitic and chloritic alterations.

In these boreholes, various minerals consisting of malachite, azurite, cuprite, smithsonite, and hemimorphite were seen in the oxidized zone.

Magnetite and iron oxides are extended in oxidation and transition zones. Malachite, native Cu and bornite hold a specific sequence at the depth.

Figure 12 illustrates the concentration distribution of Au and Cu elements in borehole DDH4. The results show a notable increasing trend for the Cu and Au grades and chalcopyrite mineral at the beginning of the hypogene zone. The Mo concentration shows a rising trend from surface to depth, and an enrichment zone of Mo was shown at the high depth. Distinctive relationships between the mineralization elements of Cu, Au, and Mo are shown based on deep investigations.

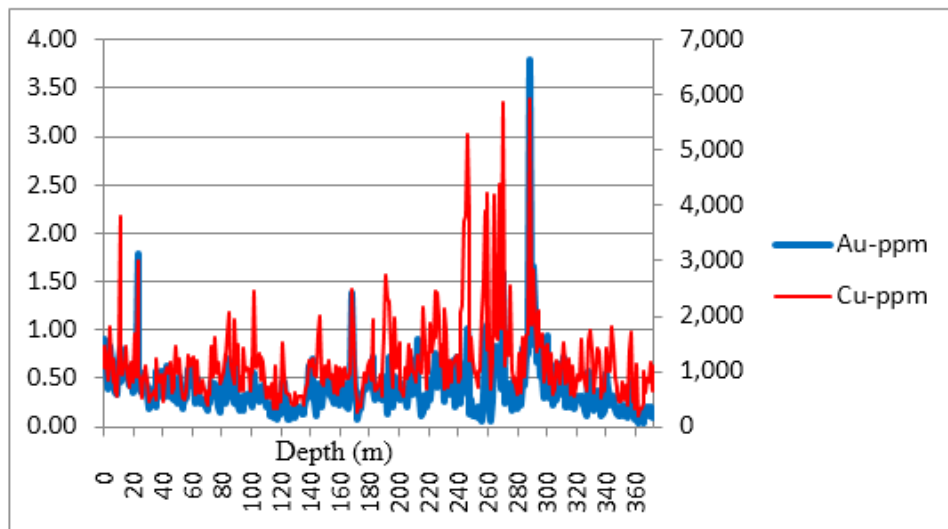


Figure 12. Concentration distribution of Au and Cu elements in Borehole DDH4.

The detailed exploration works correctly confirm the obtained geochemical map, and demonstrate that the fractal modeling of GMPI on cleaned and transformed data could be helpful for introducing the high potential targets. The hybrid approach applied in this investigation provided favorable results. It could model the geochemical distribution of paragenesis elements on the local scale based on two transformation functions of CLR and GMPI.

4.5. Correlation with specific geological evidences

There is a notable correlation between the results of the fractal model of GMPI and geological evidences, especially in mineralization zones. The significant moderate and high anomalies obtained by fractal modeling of GMPI (Cu, Au, Mo) have been extended in the central parts of the area and overlapped on quartz diorite porphyry and andesite rocks. The Dalli area

has been affected by intrusive and volcanic masses of the Tertiary period. This area is mainly covered by igneous rocks such as diorite, quartz diorite, tonalite, and andesite, which have been altered to potassic, siliceous, phillitic, argillic, and propylitic alterations under the influence of hydrothermal solutions. These solutions have caused the mineralization of copper and gold in potassic, siliceous, and phillitic alterations. The Cu and Au mineralizations are related to the quartz diorite stocks that encompass the quartz veinlets and quartz–magnetite stockwork zones. Mineralization is also shown in the contact of the quartz diorite and Andesite rocks. Petrographic studies also confirm that the quartz diorite, quartz Monzonite, and andesite units are mineralization host rocks. Chalcopyrite, bornite, chalcocite, malachite, pyrite, and iron oxide minerals are also observed in these parts. The field observations show that the potassic alteration has covered the obtained

anomaly areas with high intensity, and weak phillitic and chlorite alterations are also seen in these parts.

6. Conclusions

In this work, a hybrid approach including the C-N fractal model, PCA, and GMPI methods was performed for geochemical anomaly defining in the Dalli Cu porphyry mineralization area.

These methods were applied on the centered log-ratio transformed data, and the geochemical outliers were detected and rejected. The PCA method extracted five PCs from the cleaned and CLR transformed geochemical dataset. The paragenetic elements of Cu, Au, and Mo constructed PC1 as $MF_{(Cu, Au, Mo)}$, and then the GMPI values of this factor were calculated and modeled using the C-N fractal method. The C-N fractal modeling of GMPI ($MF_{(Cu, Au, Mo)}$) identified four geochemical populations consisting of geochemical background, and weak, moderate, and high anomalies. The promising geochemical targets delineated by this hybrid approach were adequately validated by more detailed surface exploration works and deep boreholes. The obtained multivariate anomalies are properly associated with the potassic and phillitic alterations and mineralization zones. The results demonstrate fractal modeling of GMPI values can improve the multivariate geochemical signature in geochemical mapping. The obtained results indicated that this hybrid scenario was practical for anomaly definition, and was helpful for geochemical data modeling in various exploratory stages, especially on the local scale.

References

- [1]. Carranza, E.J.M. (2008). Geochemical anomaly and mineral prospectivity mapping in GIS. Elsevier.
- [2]. Yousefi, M., Carranza, E.J.M., Kreuzer, O.P., Nykänen, V., Hronsky, J.M., and Mihalasky, M.J. (2021). Data analysis methods for prospectivity modelling as applied to mineral exploration targeting: state-of-the-art and outlook. *Journal of Geochemical Exploration*, 229, 106839.
- [3]. Seyedrahimi-Niarag, M., and Mahdiyanfar, H. (2021). Introducing a new approach of geochemical anomaly intensity index (GAIL) for increasing the probability of exploration of shear zone gold mineralization. *Geochemistry*. 81(4): 125830.
- [4]. Yousefi, M. (2017). Analysis of zoning pattern of geochemical indicators for targeting of porphyry-Cu mineralization: a pixel-based mapping approach. *Natural Resources Research*. 26 (4): 429-441.
- [5]. Plant, J.A., and Hale, M. (1994). Introduction: the foundations of modern drainage geochemistry. In *Handbook of Exploration Geochemistry* (Vol. 6, pp. 3-9). Elsevier Science BV.
- [6]. Ghasemzadeh, S., Maghsoudi, A., Yousefi, M., and Mihalasky, M.J. (2019). Stream sediment geochemical data analysis for district-scale mineral exploration targeting: Measuring the performance of the spatial U-statistic and CA fractal modeling. *Ore Geology Reviews*, 113, 103115.
- [7]. Zuo, R., and Wang, J. (2016). Fractal/multifractal modeling of geochemical data: A review. *Journal of Geochemical Exploration*, 164, 33-41.
- [8]. Salimi, A., and Rafiee, A. (2022). A grid interpolation technique for anomaly separation of stream sediments geochemical data based on catchment basin modelling, U-statistics and fractal. *Earth Science Informatics*, 15(1), 151-161.
- [9]. Yang, L., Wang, Q., and Liu, X. (2015). Correlation between mineralization intensity and fluid-rock reaction in the Xinli gold deposit, Jiaodong Peninsula, China: constraints from petrographic and statistical approaches. *Ore Geology Reviews*, 71, 29-39.
- [10]. Cheng, Q., Agterberg, F.P., and Bonham-Carter, G.F. (1996). A spatial analysis method for geochemical anomaly separation. *Journal of Geochemical exploration*. 56 (3): 183-195.
- [11]. Chen, Y.Q., Zhao, B.N., Chen, C., Zhao, B.B., and Zhao, P.D. (2022). Identification of ore-finding targets using the anomaly components of ore-forming element associations extracted by SVD and PCA in the Jiaodong gold cluster area, Eastern China. *Ore Geology Reviews*, 144, 104866.
- [12]. Yin, B., Zuo, R., Xiong, Y., Li, Y., and Yang, W. (2021). Knowledge discovery of geochemical patterns from a data-driven perspective. *Journal of Geochemical Exploration*, 231, 106872.
- [13]. Almasi, A., Jafarirad, A., Afzal, P., and Rahimi, M. (2015). Prospecting of gold mineralization in Saqez area (NW Iran) using geochemical, geophysical and geological studies based on multifractal modelling and principal component analysis. *Arabian Journal of Geosciences*. 8 (8): 5935-5947.
- [14]. Chen, Y., Zhang, L., and Zhao, B. (2019). Identification of the anomaly component using BEMD combined with PCA from element concentrations in the Tengchong tin belt, SW China. *Geoscience Frontiers*. 10 (4): 1561-1576.

- [15]. Cheng, Q., Bonham-Carter, G., Wang, W., Zhang, S., Li, W., and Qinglin, X. (2011). A spatially weighted principal component analysis for multi-element geochemical data for mapping locations of felsic intrusions in the Gejiu mineral district of Yunnan, China. *Computers and Geosciences*, 37 (5): 662-669.
- [16]. Zheng, C., Liu, P., Luo, X., Wen, M., Huang, W., Liu, G., and Albanese, S. (2021). Application of compositional data analysis in geochemical exploration for concealed deposits: A case study of Ashele copper-zinc deposit, Xinjiang, China. *Applied Geochemistry*, 130, 104997.
- [17]. Elghonimy, R., and Sonnenberg, S. (2021). A Principal Component Analysis Approach to Understanding Relationships Between Elemental Geochemistry Data and Deposition, Niobrara Formation, Denver Basin, CO. In SPE/AAPG/SEG Unconventional Resources Technology Conference. OnePetro.
- [18]. Shahi, H., Ghavami, R., and Rouhani, A.K. (2016). Detection of deep and blind mineral deposits using new proposed frequency coefficients method in frequency domain of geochemical data. *Journal of Geochemical Exploration*, 162, 29-39.
- [19]. Shahi, H., Ghavami, R., Rouhani, A.K., Kahoo, A.R., and Haroni, H.A. (2015). Application of Fourier and wavelet approaches for identification of geochemical anomalies. *Journal of African Earth Sciences*, 106, 118-128.
- [20]. Shahi, H., Ghavami, R., and Rouhani, A.K. (2016). Comparison of mineralization pattern of geochemical data in spatial and position-scale domain using new DWT-PCA approach. *Journal of the Geological Society of India*. 88 (2): 235-244.
- [21]. Yousefi, M., Kamkar-Rouhani, A., and Carranza, E.J.M. (2012). Geochemical mineralization probability index (GMPI): a new approach to generate enhanced stream sediment geochemical evidential map for increasing probability of success in mineral potential mapping. *Journal of Geochemical Exploration*, 115, 24-35.
- [22]. Afzal, P., Yousefi, M., Mirzaie, M., Ghadiri-Sufi, E., Ghasemzadeh, S., and Daneshvar Saein, L. (2019). Delineation of podiform-type chromite mineralization using geochemical mineralization prospectivity index and staged factor analysis in Balvard area (SE Iran). *Journal of Mining and Environment*. 10 (3): 705-715.
- [23]. Yousefi, M., Kamkar-Rouhani, A., and Carranza, E. J. M. (2014). Application of staged factor analysis and logistic function to create a fuzzy stream sediment geochemical evidence layer for mineral prospectivity mapping. *Geochemistry: Exploration, Environment, Analysis*. 14 (1): 45-58.
- [24]. Yousefi, M., and Carranza, E.J.M. (2015). Fuzzification of continuous-value spatial evidence for mineral prospectivity mapping. *Computers and Geosciences*, 74, 97-109.
- [25]. Yousefi, M., and Carranza, E.J.M. (2017). Union score and fuzzy logic mineral prospectivity mapping using discretized and continuous spatial evidence values. *Journal of African Earth Sciences*, 128, 47-60.
- [26]. Saadati, H., Afzal, P., Torshizian, H., and Solgi, A. (2020). Geochemical exploration for lithium in NE Iran using the geochemical mapping prospectivity index, staged factor analysis, and a fractal model. *Geochemistry: Exploration, Environment, Analysis*, 20(4), 461-472.
- [27]. Cheng, Q. (1999). Spatial and scaling modelling for geochemical anomaly separation. *Journal of Geochemical Exploration*. 65 (3): 175-194.
- [28]. Goncalves, M.A., Mateus, A., and Oliveira, V. (2001). Geochemical anomaly separation by multifractal modelling. *Journal of Geochemical Exploration*. 72 (2): 91-114.
- [29]. Sim, B.L., Agterberg, F.P., and Beaudry, C. (1999). Determining the cutoff between background and relative base metal smelter contamination levels using multifractal methods. *Computers and Geosciences*. 25 (9): 1023-1041.
- [30]. Ouchchen, M., Boutaleb, S., Abia, E.H., El Azzab, D., Miftah, A., Dadi, B. and Abioui, M. (2022). Exploration targeting of copper deposits using staged factor analysis, geochemical mineralization prospectivity index, and fractal model (Western Anti-Atlas, Morocco). *Ore Geology Reviews*, 143, 104762.
- [31]. Agterberg, F.P. (1996). Multifractal modelling of the sizes and grades of giant and supergiant deposits. *Global tectonics and metallogeny*, 131-136.
- [32]. Mao, Z., Peng, S., Lai, J., Shao, Y., and Yang, B. (2004). Fractal study of geochemical prospecting data in south area of Fenghuanshan copper deposit, Tongling Anhui. *Journal of Earth Sciences and Environment*. 26 (4): 11-14.
- [33]. Ghannadpour, S.S., and Hezarkhani, A. (2022). Delineation of geochemical anomalies for mineral exploration using combining U-statistic method and fractal technique: UN and UA models. *Applied Earth Science*. 131 (1): 32-48.
- [34]. Cheng, Q., Agterberg, F.P., and Ballantyne, S.B. (1994). The separation of geochemical anomalies from background by fractal methods. *Journal of Geochemical Exploration*. 51 (2): 109-130.
- [35]. Khammar, F., Yousefi, S., and Joonaghani, S.A. (2021). Analysis of litho-geochemical data using log-ratio transformations and CA fractal to separate geochemical

anomalies in Tak-Talar, Iran. *Arabian Journal of Geosciences*. 14 (8): 1-15.

[36]. Li, C., Ma, T., and Shi, J. (2003). Application of a fractal method relating concentrations and distances for separation of geochemical anomalies from background. *Journal of Geochemical exploration*. 77 (2-3): 167-175.

[37]. Cheng, Q., Xu, Y., and Grunsky, E. (2000). Integrated spatial and spectrum method for geochemical anomaly separation. *Natural Resources Research*. 9 (1): 43-52.

[38]. Koohzadi, F., Afzal, P., Jahani, D., and Pourkermani, M. (2021). Geochemical exploration for Li in regional scale utilizing Staged Factor Analysis (SFA) and Spectrum-Area (SA) fractal model in north central Iran. *Iranian Journal of Earth Sciences*. 13(4): 299-307.

[39]. Mahdiyfar, H. (2020). Prediction of economic potential of deep blind mineralization by Fourier transform of a geochemical dataset. *Periodico di Mineralogia*. 90 (1).

[40]. Heidari, S.M., Afzal, P., Ghaderi, M., and Sadeghi, B. (2021). Detection of mineralization stages using zonality and multifractal modeling based on geological and geochemical data in the Au-(Cu) intrusion-related Gouzal-Bolagh deposit, NW Iran. *Ore Geology Reviews*, 139, 104561.

[41]. Afzal, P., Alghalandis, Y.F., Khakzad, A., Moarefvand, P., and Omran, N.R. (2011). Delineation of mineralization zones in porphyry Cu deposits by fractal concentration-volume modeling. *Journal of Geochemical exploration*. 108 (3): 220-232.

[42]. Afzal, P., Farhadi, S., Boveiri Konari, M., Shamseddin Meigooni, M., and Daneshvar Saein, L. (2022). Geochemical anomaly detection in the Irankuh District using Hybrid Machine learning technique and fractal modeling. *Geopersia*.

[43]. Farhadi, S., Afzal, P., Boveiri Konari, M., Daneshvar Saein, L., and Sadeghi, B. (2022). Combination of Machine Learning Algorithms with Concentration-Area Fractal Method for Soil Geochemical Anomaly Detection in Sediment-Hosted Irankuh Pb-Zn Deposit, Central Iran. *Minerals*. 12 (6): 689.

[44]. Hassanpour, S., and Afzal, P. (2013). Application of concentration-number (C-N) multifractal modeling for geochemical anomaly separation in Haftcheshmeh porphyry system, NW Iran. *Arabian Journal of Geosciences*. 6 (3): 957-970.

[45]. Shahbazi, S., Ghaderi, M., and Afzal, P. (2021). Prognosis of gold mineralization phases by multifractal modeling in the Zehabad epithermal deposit, NW Iran. *Iranian Journal of Earth Sciences*. 13 (1): 31-40.

[46]. Leung, R., Balamurali, M., and Melkumyan, A. (2021). Sample truncation strategies for outlier removal in geochemical data: the MCD robust distance approach versus t-SNE ensemble clustering. *Mathematical Geosciences*. 53 (1): 105-130.

[47]. Garrett, R.G., Reimann, C., Hron, K., Kynčlová, P., and Filzmoser, P. (2017). Finally, a correlation coefficient that tells the geochemical truth. *Explore*, 176, 1-10.

[48]. Shafiei, B., Haschke, M., and Shahabpour, J. (2009). Recycling of orogenic arc crust triggers porphyry Cu mineralization in Kerman Cenozoic arc rocks, southeastern Iran. *Mineralium Deposita*. 44 (3): 265-283.

[49]. Waterman, G.C., and Hamilton, R.L. (1975). The Sar Cheshmeh porphyry copper deposit. *Economic Geology*. 70 (3): 568-576.

[50]. Asadi, H.H., Porwal, A., Fatehi, M., Kianpouryan, S., and Lu, Y.J. (2015). Exploration feature selection applied to hybrid data integration modeling: Targeting copper-gold potential in central Iran. *Ore Geology Reviews*, 71, 819-838.

[51]. Ayati, F., Yavuz, F., Asadi, H.H., Richards, J.P., and Jourdan, F. (2013). Petrology and geochemistry of calc-alkaline volcanic and subvolcanic rocks, Dalli porphyry copper-gold deposit, Markazi Province, Iran. *International Geology Review*. 55 (2): 158-184.

[52]. Asadi Haroni, H. (2008). First stage drilling report on Dalli porphyry Cu-Au prospect, Central Province of Iran. *Technical of Iran, Isfahan, Report, 1, 24*.

[53]. Asadi, H.H. (2008). Final exploration report of Dalli porphyry Cu-Au deposit. Markazi province. *Technical Report. Dorsa Pardazeh Company, Isfahan, Report 01*.

[54]. Aitchison, J. (1982). The statistical analysis of compositional data. *Journal of the Royal Statistical Society: Series B (Methodological)*. 44 (2): 139-160.

[55]. Carranza, E.J.M. (2011). Analysis and mapping of geochemical anomalies using logratio-transformed stream sediment data with censored values. *Journal of Geochemical Exploration*. 110 (2): 167-185.

[56]. Graffelman, J., Pawlowsky-Glahn, V., Egozcue, J.J., and Buccianti, A. (2018). Exploration of geochemical data with compositional canonical biplots. *Journal of geochemical exploration*, 194, 120-133.

[57]. Filzmoser, P., and Hron, K. (2008). Outlier detection for compositional data using robust methods. *Mathematical Geosciences*. 40 (3): 233-248.

[58]. Owen, D.D.R., Pawlowsky-Glahn, V., Egozcue, J.J., Buccianti, A., and Bradd, J.M. (2016). Compositional data analysis as a robust tool to delineate hydrochemical facies within and between gas-bearing aquifers. *Water Resources Research*. 52 (8): 5771-5793.

- [59]. Begashaw, G.B., and Yohannes, Y.B. (2020). Review of outlier detection and identifying using robust regression model. *International Journal of Systems Science and Applied Mathematics*. 5 (1): 4-11.
- [60]. Filzmoser, P., Reimann, C., and Garrett, R. G. (2004). A multivariate outlier detection method (pp. 18-22). na.
- [61]. Rousseeuw, P.J., and Van Zomeren, B. C. (1990). Unmasking multivariate outliers and leverage points. *Journal of the American Statistical association*. 85 (411): 633-639.
- [62]. Farzamian, M., Rouhani, A. K., Yarmohammadi, A., Shahi, H., Sabokbar, H. A., and Ziaie, M. (2016). A weighted fuzzy aggregation GIS model in the integration of geophysical data with geochemical and geological data for Pb–Zn exploration in Takab area, NW Iran. *Arabian Journal of Geosciences*. 9 (2): 1-17.
- [63]. Mahdiyanfar, H. (2020). A Critique on Power Spectrum–Area Fractal Method for Geochemical Anomaly Mapping. *Journal of Analytical and Numerical Methods in Mining Engineering*. 10 (25): 33-41.
- [64]. Mahdiyanfar, H. (2021). Identification of Buried Metal Ore Deposits using Geochemical Anomaly Filtering and Principal Factors of Power Spectrum. *Journal of Mining and Environment*. 12 (1): 205-218.
- [65]. Seyedrahimi-Niaraq, M., Mahdiyanfar, H., and Mokhtari, A.R. (2022). Integrating principal component analysis and U-statistics for mapping polluted areas in mining districts. *Journal of Geochemical Exploration*, 234, 106924.
- [66]. Afzal, P., Mirzaei, M., Yousefi, M., Adib, A., Khalajmasoumi, M., Zarifi, A. Z. and Yasrebi, A.B. (2016). Delineation of geochemical anomalies based on stream sediment data utilizing fractal modeling and staged factor analysis. *Journal of African Earth Sciences*, 119, 139-149.

شناسایی ناهنجاری‌های ژئوشیمیایی با استفاده از مدل سازی فرکتالی داده‌های GMPI حاصله از داده‌های ژئوشیمیایی تبدیل یافته لگاریتمی میان مرکز مطالعه موردی: کانی‌سازی مس پورفیری

حسین مهديان فر^{۱*} و امير سليمي^۲

۱. گروه مهندسی معدن، مجتمع آموزش عالی گناباد، گناباد، ایران
 ۲. گروه مهندسی معدن، دانشکده مهندسی، دانشگاه زنجان، زنجان، ایران

ارسال ۲۰۲۲/۰۵/۲۱، پذیرش ۲۰۲۲/۰۹/۰۷

* نویسنده مسئول مکاتبات: hssn.mahdiyanfar@gmail.com

چکیده:

هدف از این تحقیق شناسایی شاخص‌های ژئوشیمیایی در کانسار مس پورفیری دالی با استفاده از نمونه‌های ژئوشیمیایی برداشت شده از محیط خاک است. در گام نخست، داده‌های ژئوشیمیایی با استفاده از روش تبدیل لگاریتمی میان مرکز (CLR) باز شدند. سپس نمونه‌های خارج از ردیف و پرت که دقت مدل‌های ژئوشیمیایی را کاهش می‌دهند با استفاده از روش فاصله ماهالانویس شناسایی و حذف گردیدند. در ادامه روش‌های آنالیز مؤلفه اصلی (PCA) و شاخص GMPI بر روی مجموعه داده‌های ژئوشیمیایی تبدیل‌یافته و پاک شده از داده‌های پرت اعمال شدند. روش PCA موفق به شناسایی ۵ مؤلفه اصلی گردید که از میان آنها مؤلفه اول که شامل مس، طلا و مولیبدن است به عنوان فاکتور کانی سازی (MF) انتخاب شد. روش GMPI می‌تواند شاخص‌های ژئوشیمیایی چند متغیره را در نقشه برداری ژئوشیمیایی را بهبود دهد. از این رو مقادیر GMPI نمونه‌ها بر اساس مقادیر فاکتور کانی سازی عناصر مس، طلا و مولیبدن محاسبه گردید. نتایج بدست آمده نشان داد که مقادیر بزرگ GMPI به شدت با سنگ‌های پورفیری کوارتز دیوریت و مناطق دگرسانی پتاسیک همبستگی دارد. مدل‌سازی شاخص (MF) GMPI (Cu, Au, Mo) با استفاده از روش هند سه فرکتالی عیار-عدد (C-N) انجام گرفت. مدل فرکتالی عیار-تعداد چهار جامعه ژئوشیمیایی بر اساس ابعاد فرکتالی مختلف شناسایی کرد. نقشه ناهنجاری ژئوشیمیایی (MF) GMPI (Cu, Au, Mo) بر اساس ۴ جمعیت مذکور ترسیم گردید. مناطق امید بخش بدست آمده بوسیله کارهای اکتشافی تفصیلی‌تر و همچنین حفاری‌های عمیق مورد اعتبارسنجی قرار گرفت. بخش‌های با پتانسیل کانی‌سازی مس-طلا به صورت مناسبی با استفاده از این روش ترکیبی مشخص گردید. نتایج بدست‌آمده نشان می‌دهد که این روش به صورت موفقیت آمیزی می‌تواند برای نقشه‌برداری ژئوشیمیایی در مقیاس‌های محلی مورد استفاده قرار گیرد.

کلمات کلیدی: نقشه برداری ناهنجاری ژئوشیمیایی، تشخیص داده‌های خارج از ردیف، مدل سازی فرکتالی، مدل ژئوشیمیایی.